Acta Crystallographica Section B
Structural Science
ISSN 0108-7681

Structure of N^6-furfurylaminopurine (kinetin) dihydrogenphosphate

G. Ślósarek,[a]* M. Kozak,[b] J. Gierszewski[a] and A. Pietraszko[c]

[a]Department of Molecular Biophysics, Faculty of Physics, Adam Mickiewicz University, Poznań, Poland, [b]Department of Macromolecular Physics, Faculty of Physics, Adam Mickiewicz University, Poznań, Poland, and [c]Institute of Low Temperature and Structure Research, Polish Academy of Sciences, Wrocław, Poland

Correspondence e-mail: leonardo@main.amu.edu.pl

Received 29 March 2005
Accepted 22 August 2005

The crystal structure of kinetin dihydrogenphosphate has been determined at 115 and 293 K. Kinetin dihydrogenphosphate undergoes a polymorphic phase transition at 291.1 K. In both phases the crystal belongs to the triclinic system with the symmetry described by the space group $P\bar{1}$. In the low-temperature phase, the unit cell is doubled along the *a* axis. There is a dynamic equilibrium between different tautomeric forms of the adenine residue, determined by the distribution of H atoms within the network of hydrogen bonds.

1. Introduction

Kinetin (N^6-furfurylaminopurine) was isolated for the first time from herring sperm DNA (Miller *et al.*, 1955, 1956). The molecule is classified as a cytokinin, a plant hormone. Its biological activity is related to gene expression, the inhibition of auxin action, the stimulation of calcium flux and the course of the cell cycle (Barciszewski *et al.*, 1999, 2000).

The molecular and crystal structure of kinetin have been previously analysed. Soriano-Garcia & Parthasarathy (1977) presented the crystal structure analysis of kinetin. These experimental results together with the crystal structure analyses of other cytokinins have been used for the determination of the molecular characteristics of cytokinins (Korszun *et al.*, 1989). One of the most important features of this group of molecules is their conformation around the nitrogen–carbon bond connecting the adenine residue with the proper aliphatic or aromatic residue. Similar studies have been performed for the copper complex of kinetin (Parvez & Birdsall, 1990) as well as for kinetin hydrochlorate (Stanley *et al.*, 2003).

In the following we present the results of the crystal structure analysis of kinetin dihydrogenphosphate based on the experimental data obtained at 115 and 293 K. We observed that at low temperatures the crystal underwent a structural phase transition. The transformation was manifested by the doubling of the volume of the unit cell. As we shall present in the following, the mechanism of this transition is related to the redistribution of H atoms within the hydrogen-bond network as well as the change in tautomeric form of the adenine residue.

2. Experiment

Kinetin (99%) was purchased from Sigma-Aldrich. Orthophosphoric acid (85%, spectrally pure) was purchased from POCH Gliwice SA, Poland.

In order to obtain crystals of kinetin dihydrogenphosphate we prepared a water suspension of kinetin since the solubility

Table 1
Experimental data.

	115 K	293 K
Crystal data		
Chemical formula	$C_{10}H_{12}N_5O_5P$	$C_{10}H_9N_5O{\cdot}H_3O_4P$
M_r	313.22	313.22
Cell setting, space group	Triclinic, $P\bar{1}$	Triclinic, $P\bar{1}$
a, b, c (Å)	8.9243 (18), 10.720 (2), 14.295 (3)	4.4923 (9), 10.736 (2), 14.455 (3)
α, β, γ (°)	91.41 (3), 100.75 (3), 108.85 (3)	91.00 (3), 100.92 (3), 108.47 (3)
V (Å^3)	1266.2 (4)	647.0 (2)
Z	4	2
D_x (Mg m^{-3})	1.643	1.608
Radiation type	Mo $K\alpha$	Mo $K\alpha$
No. of reflections for cell parameters	5624	3615
θ range (°)	1.30–4.07	2.16–20.13
μ (mm^{-1})	0.25	0.25
Temperature (K)	115 (2)	293 (2)
Crystal form, colour	Thin needle, colourless	Thin needle, colourless
Crystal size (mm)	0.41 × 0.09 × 0.09	0.41 × 0.09 × 0.09
Data collection		
Diffractometer	KM4CCD	KM4CCD
Data collection method	CCD	CCD
Absorption correction	Analytical *CrysAlis*, Version 170.26	Analytical *CrysAlis*, Version 170.26
T_{min}	0.910	0.915
T_{max}	0.982	0.982
No. of measured, independent and observed reflections	11 933, 5604, 5604	14 205, 5349, 3704
Criterion for observed reflections	$I > 2\sigma(I)$	$I > 2\sigma(I)$
R_{int}	0.049	0.042
θ_{max} (°)	28.1	40.3
Range of h, k, l	$-9 \Rightarrow h \Rightarrow 11$ $-14 \Rightarrow k \Rightarrow 13$ $-18 \Rightarrow l \Rightarrow 18$	$-5 \Rightarrow h \Rightarrow 8$ $-17 \Rightarrow k \Rightarrow 19$ $-24 \Rightarrow l \Rightarrow 25$
Refinement		
Refinement on	F^2	F^2
$R[F^2 > 2\sigma(F^2)]$, $wR(F^2)$, S	0.043, 0.119, 1.22	0.056, 0.122, 1.21
No. of reflections	5604	3704
No. of parameters	451	230
H-atom treatment	Mixture of independent and constrained refinement	Mixture of independent and constrained refinement
Weighting scheme	$w = 1/[\sigma^2(F_o^2) + (0.040P)^2 + 0.3P]$, where $P = (F_o^2 + 2F_c^2)/3$	$w = 1/[\sigma^2(F_o^2) + (0.030P)^2 + 0.1P]$, where $P = (F_o^2 + 2F_c^2)/3$
$(\Delta/\sigma)_{max}$	0.366	1.110
$\Delta\rho_{max}$, $\Delta\rho_{min}$ (e Å^{-3})	0.66, −0.49	0.42, −0.41
Extinction method	*SHELXL*	*SHELXL*
Extinction coefficient	0.00000 (19)	0.0051 (6)

of this compound in pure water is very low (Krzaczkowska *et al.*, 2004). Excess orthophosphoric acid was then added (molar ratio of kinetin-to-dihydrogenphosphate *ca* 1:5), which strongly increased the solubility of kinetin. The final solution was concentrated by heating followed by evaporation. Crystals of kinetin dihydrogenphosphate, in the form of long thin needles, were grown in 3 d. The quality of the single crystals was not perfect, but sufficiently good for X-ray investigation.

Single-crystal X-ray diffraction data were collected using an automatic X-ray four-circle KUMA Diffraction diffractometer with CCD area detector. Graphite-monochromated Mo $K\alpha$ radiation was generated at 50 kV and 25 mA. Each image for a 1° rotation around the ω axis was obtained in 30 s. The intensities of the reflections were recorded in 1200 frames. The temperature was regulated and stabilized with the accuracy of 0.5 K using an Oxford Cryo-system. The temperature dependence of the lattice parameters and the intensity of selected reflections were measured over the range 115–295 K. Details of data collection and structure refinement are presented in Table 1.

The crystal structure both at low (115 K) and high (293 K) temperature was solved using the direct method (*SHELXL*97; Sheldrick, 1997). The same program was used for the successive refinement cycles of the crystal structure.

Differential scanning calorimetry (DSC) measurements were performed on an DSC-204 apparatus made by Netzsch. The samples of 4 mg ± 5% were closed in aluminium crucibles with pierced lids. Prior to measuring, the samples were thermally equilibrated at 223 K for 10 min and the measurements (223–373 K) were performed at the heating rate of 5 K min^{-1} in helium. Three independent measurements were performed and the results were averaged. The data were analysed using the program *TA* (Netzsch).

3. Results and discussion

3.1. Crystal structure and structural transformation

At 293 K the unit cell of the crystal of kinetin dihydrogenphosphate contains one crystallographically independent cation of kinetin and one dihydrogenphosphate anion in the asymmetric unit. The diagram of both ions together with the atom-labelling scheme is shown in Fig. 1(*a*). The arrangement of the ions in the unit cell of the crystal is presented in Fig. 2.

There is no pairing between kinetin cations, as observed in the kinetin crystal (Soriano-Garcia & Parthasarathy, 1977). However, kinetin forms dimers, where two adenine residues are bound together by a strong N9*A*—H9*A*···N9*A* hydrogen bond, which at 293 K is characterized by the bond length 2.8837 Å and the angle 173.9° (Table 2). There are also dimers of dihydrogenphosphate groups joined together by the hydrogen bond O12—H12···O12 [$d(D\cdots A) = 2.5435$ Å, angle $(DHA) = 162°$]. At room temperature, the atoms within both these hydrogen bonds are coupled by a centre of symmetry

Table 2
Geometry of the hydrogen bonds.

D—H···A	$d(D$—H) (Å)	d(H···A) (Å)	$d(D\cdots A)$ (Å)	D—H···A (°)
Temperature 115 K				
Kinetin *A*				
N3*A*—11H3*A*···O13	1.10 (3)	1.45 (3)	2.545 (2)	174 (2)
N6*A*—H6*A*···O21^{i}	0.847 (19)	2.02 (2)	2.8582 (19)	168.4 (18)
N7*A*—H7*A*···O21^{i}	0.93 (2)	1.91 (2)	2.778 (2)	153.8 (17)
Kinetin *B*				
O23—H23···N3*B*	1.04 (3)	1.61 (3)	2.637 (2)	171 (2)
N6*B*—H6*B*···O11^{ii}	0.832 (19)	2.086 (19)	2.9051 (19)	168.5 (18)
N7*B*—H7*B*···O11 ^{ii}	0.92 (2)	1.80 (2)	2.671 (2)	158.7 (17)
N9*B*—H9*B*···N9*A*^{iii}	1.04 (3)	1.83 (3)	2.872 (2)	175 (2)
Dihydrogenphosphate				
O12—H12···O21	0.74 (3)	1.80 (3)	2.5438 (18)	178 (3)
O24—H24···O11^{iv}	0.75 (3)	1.80 (3)	2.5476 (18)	176 (3)
O14—H14···O22^{v}	1.06 (3)	1.49 (3)	2.5410 (19)	178 (2)
Temperature 293 K				
N9*A*—H9*A*···N9*A*^{vi}	0.843 (15)	2.044 (16)	2.8837 (19)	173.9 (15)
O12—H12···O12^{v}	0.85 (2)	1.72 (2)	2.5435 (17)	162 (3)
N3*A*—H3···O13^{vi}	1.193 (19)	1.388 (19)	2.5777 (14)	174.4 (17)
O14—H14···O11^{vii}	0.818 (13)	1.734 (13)	2.5501 (12)	174.9 (12)
N6*A*—H6*A*···O11^{viii}	0.886 (12)	2.030 (12)	2.9019 (13)	168.0 (10)
N7*A*—H7*A*···O11^{viii}	0.992 (12)	1.825 (11)	2.7414 (13)	152.2 (11)

Symmetry codes: (i) $x, y+1, z$; (ii) $x+1, y+1, z$; (iii) $-x+1, -y+2, -z+1$; (iv) $x+1, y, z$; (v) $-x+1, -y+1, -z+1$; (vi) $-x+1, -y, -z+1$; (vii) $x-1, y, z$; (viii) $-x+2, -y+1, -z+1$.

and the H atoms occupy two symmetrically equivalent positions. There is also a mutual interaction between the two dimers through the hydrogen bond N3*A*—H3···O13 [$d(D\cdots A)$ = 2.5777 Å, angle (DHA) = 174.4°]. This interaction completes a ribbon-like network of hydrogen bonds parallel to the *b* axis.

Both kinetin and dihydrogenphosphate dimers form columns down the crystal *a* axis, which is parallel to the needle growth direction. Dihydrogenphosphate dimers are joined together down the *a* axis by a pair of O14—H14···O11 hydrogen bonds [$d(D\cdots A)$ = 2.5501 Å, angle (DHA) = 174.9°]. Each dihydrogenphosphate group in the dimer forms a separate bond with a corresponding $H_2PO_4^-$ group in the dimer from the unit cell directly below. There are also hydrogen bonds, which join the N6*A* and N7*A* atoms with the O11 atom from the dihydrogenphosphate group in the unit cell directly above.

The furfural ring of the kinetin cation is the only fragment which is not involved in the intermolecular interactions. We have observed large displacement factors for three of the furfural ring atoms: C13*A*, C14*A* and O15*A*, which indicates a strong rotational motion around the C11*A*—C12*A* bond direction.

At low temperature (115 K) the unit cell of the crystal contains two crystallographically independent formula units of kinetin dihydrogenphosphate in the asymmetric unit. We have labelled the kinetin cations with the letters *A* and *B* and the dihy-

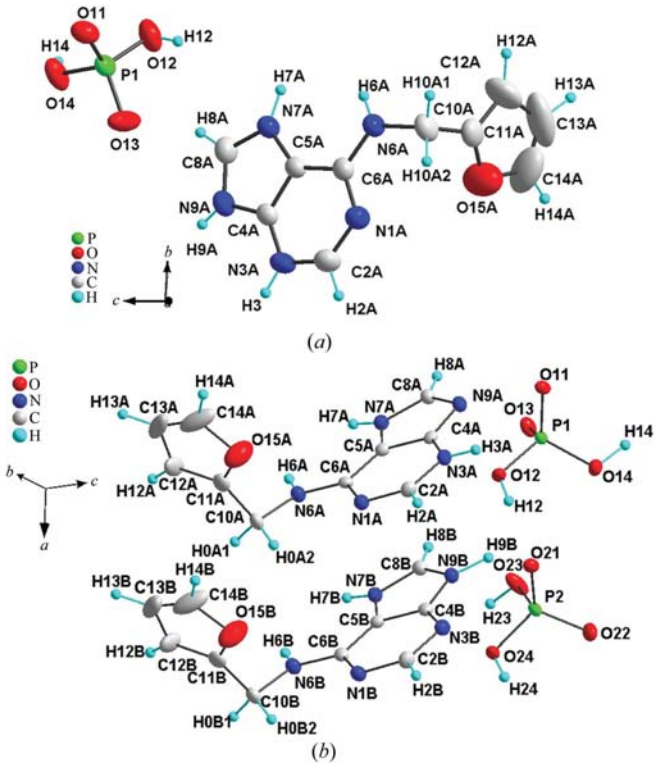

Figure 1
Diagram of kinetin and dihydrogenphosphate ions, with atom labelling: (*a*) high-temperature phase; (*b*) low-temperature phase.

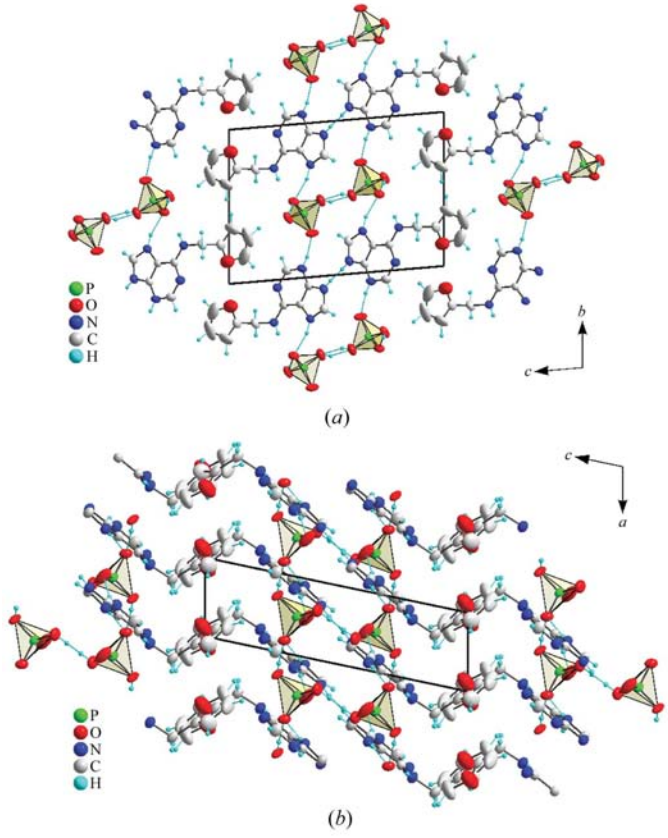

Figure 2
Projection of the crystal structure along (*a*) the *a* axis and (*b*) the *b* axis (temperature 293 K).

drogenphosphate groups with numbers 1 and 2 (Fig. 1*b*). The spatial arrangement of the ions (Fig. 3) as well as the crystallographic system (triclinic) and the space group ($P\bar{1}$) are preserved. While decreasing the temperature of the crystal, the distribution of H atoms in the hydrogen-bond network also undergoes gradual modification. Among others the potential well of the N9*B*—H9*B*···N9*A* and O12—H12···O21 hydrogen bonds becomes more and more asymmetric. This process results in the differentiation of kinetin and dihydrogenphosphate ions within the dimers and finally the doubling of the unit cell along the *a* axis. However, the overall structure of the hydrogen-bond network remains unchanged at low temperature.

The increase in the unit-cell volume is proved experimentally by the appearance of additional, superstructure reflections such as 3 −6 −1 and −3 0 3 (which correspond to 1.5 −6 −1 and −1.5 0 3 at room temperature). The intensity of these reflections (see *e.g.* Fig. 4) increases with decreasing temperature. On the basis of these data, we can estimate the transition-point temperature as 295 K. There are no sudden changes in the lattice parameters (Fig. 5). The temperature dependence of the lattice parameters and intensity of the superstructure reflections show that a continuous phase transition (second-order type) takes place in the crystal. We have performed additional measurements of the crystal structure at 15 K (Exalibur diffractometer with a HELIJET helium cryogenic attachment; a complete data file for these measurements is deposited in the Cambridge Structural Database). The refinement of the crystal structure at 15 K confirmed the crystal structure characteristics in the low-temperature (115 K) phase.

Fig. 6 presents a fragment of the DSC curve which covers a small temperature range in the vicinity of the phase transition. The process takes place within the temperature range 284–298 K (taken as the onset and endpoint temperature, respectively), with a maximum at 291.1 K. The phase transition is characterized by $\Delta H = -300.69 \pm 12.53$ J mol^{-1}.

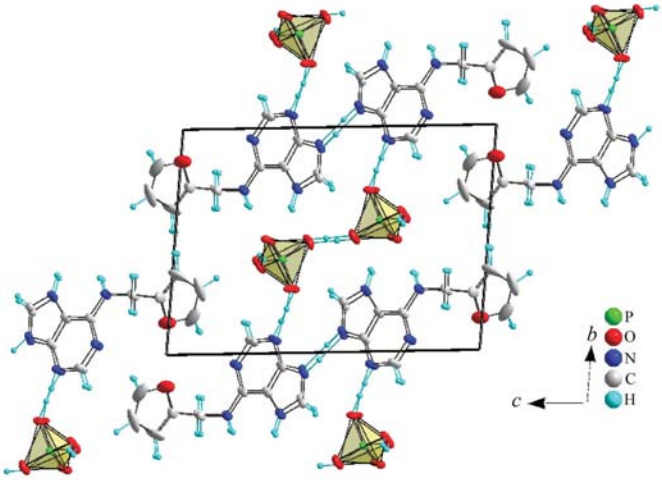

Figure 3
Projection of the crystal structure along the *a* axis (temperature 115 K).

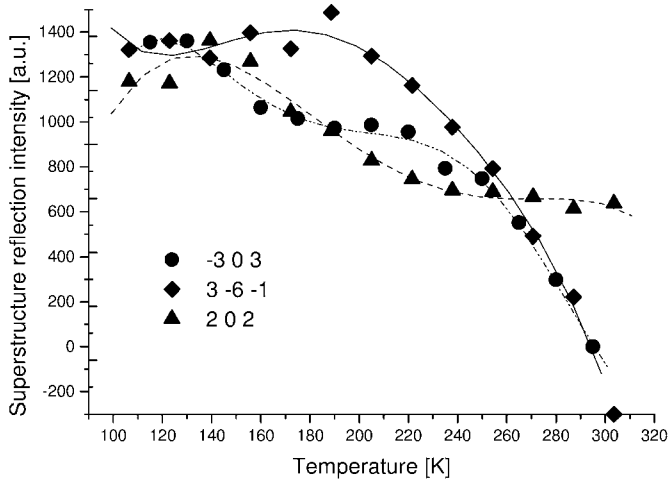

Figure 4
Temperature dependence of the superstructure reflections −3 0 3 and 3 −6 −1 from the crystal of kinetin dihydrogenphosphate.

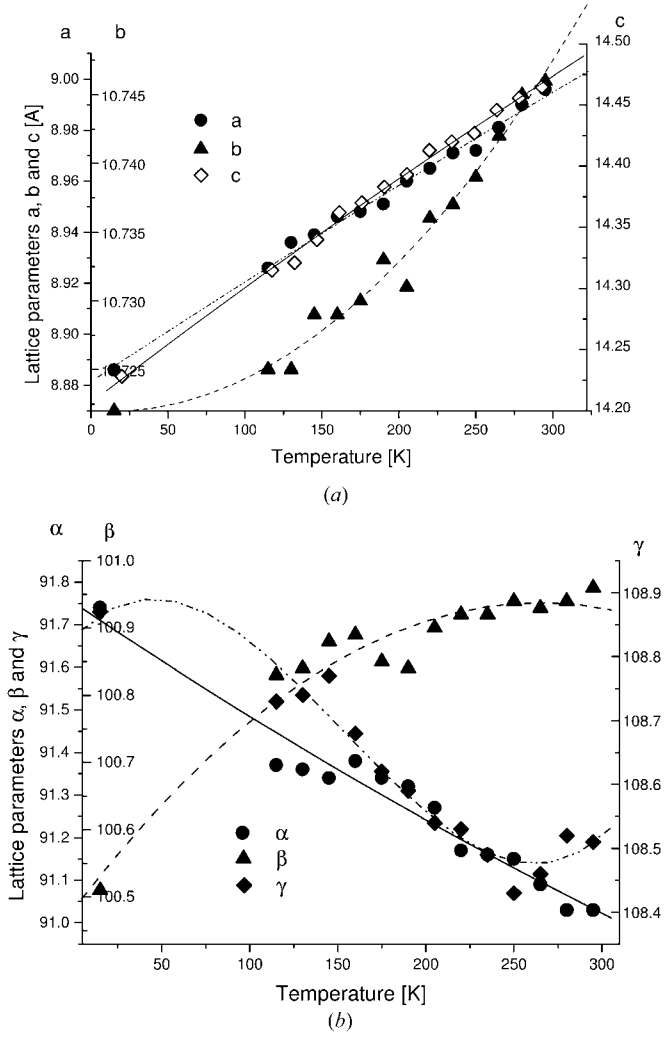

Figure 5
Temperature dependence of the unit-cell parameters: (*a*) *a*, *b* and *c*; (*b*) α, β and γ.

Table 3
Parameters (Å, °) characterizing the tautomeric form of the adenine residue.

Parameter	9*H*-Amino[(a)]	9*H*-Amino N1 protonated[(b)]	7*H*-Amino[(c)]	7*H*-Amino N3 protonated[(d)]	7*H*-Amino N3 protonated[(e)]	Doubly protonated[(f)]	Kinetin *A* temperature 115 K[(g)]	Kinetin *B* temperature 115 K	Kinetin temperature 293 K
N1—C2	1.332	1.344	1.336	1.318	1.319	1.361	1.323 (2)	1.340 (2)	1.3242 (14)
N1—C6	1.346	1.367	1.331	1.352	1.364	1.358	1.360 (2)	1.349 (2)	1.3555 (13)
C2—N3	1.315	1.307	1.324	1.342	1.333	1.302	1.339 (2)	1.345 (2)	1.3346 (15)
N3—C4	1.349	1.359	1.328	1.348	1.370	1.348	1.360 (2)	1.345 (2)	1.3528 (13)
C5—N7	1.388	1.378	1.365	1.384	1.368	1.377	1.379 (2)	1.386 (2)	1.3822 (13)
N7—C8	1.297	1.317	1.350	1.321	1.353	1.320	1.346 (2)	1.326 (2)	1.3309 (13)
C4—N9	1.370	1.369	1.387	1.350	1.346	1.372	1.370 (2)	1.383 (2)	1.3683 (14)
C8—N9	1.365	1.370	1.313	1.334	1.341	1.335	1.334 (2)	1.340 (2)	1.3344 (14)
C2—N1—C6	118.6	123.5	118.2	119.3	119.5	124.0	119.21 (15)	119.08 (15)	118.57 (9)
C2—N3—C4	111.0	111.8	111.9	118.2	118.4	112.6	116.08 (14)	112.30 (15)	113.87 (8)
C5—N7—C8	103.8	104.5	106.7	107.4	106.4	108.8	106.14 (14)	107.88 (14)	106.79 (8)
C4—N9—C8	105.7	105.9	103.2	103.5	102.6	180.5	103.54 (14)	107.64 (15)	105.61 (9)

References: (*a*) Voet & Rich (1970); (*b*) Shieh & Voet (1975); (*c*) Raghunathan & Pattabhi (1981); (*d*) Umadevi *et al.* (2001); (*e*) Stanley *et al.* (2003); (*f*) Kistenmacher & Shigematsu (1974*b*); (*g*) present data.

3.2. The structure of the kinetin cation

There are eight structural isomers of adenine (Fig. 7), which differ in the arrangement of the H atoms bound to the N atoms of the adenine ring. According to the results of the transient light absorption study in water solution at room temperature there are two isomers of adenine present: 7*H*-amino (about 22%) and 9*H*-amino (about 78% present); see Cohen *et al.* (2003). Under acidic conditions, the adenine molecule undergoes protonation. In the 9*H*-amino form an additional H atom is bound to the N1 atom, while in the 7*H*-amino tautomer the H atom is bound to the N3 atom. In the crystals of simple adenine salts such as adeninium hydrochloride (Kistenmacher & Shigematsu, 1974*a*), adeninium hydrobromide (Langer & Huml, 1978*b*), adeninium nitrate (Hingerty *et al.*, 1981), adeninium sulfate (Langer & Huml, 1978*a*; Langer *et al.*, 1978) or adeninium dihydrogenphosphate (Langer *et al.*, 1979) there is a 9*H*-amino isomer protonated at the N1 atom.

In modified adenine molecules, such as the cytokinins, the distribution of tautomers can be different. In the crystals of N^6 substituted adenine molecules such as kinetin and N^6-benzyladenine, the adenine residue takes the form of the 9*H*-amino tautomer. However, under acidic conditions, a transition from the tautomeric 9*H*-amino form to the 7*H*-amino form takes place. The experimental evidence for such a transformation could be found for crystals of kinetin hydrochloride (Stanley *et al.*, 2003), N^6-benzyladenine hydrobromide (Umadevi *et al.*, 2001) and N^6-benzyladenine cooper complex (Balasubramanian *et al.*, 1996).

The transformation of tautomeric forms is related to the deformation of adenine rings – changes in the lengths of selected bonds and the values of selected angles within the adenine rings are observed (Taylor & Kennard, 1982). Let us compare these bond lengths and angles around the N atoms in an adenine molecule and the adenine residue in kinetin dihydrogenphosphate. The data are presented in Table 3. In the first six columns we present the data known from the literature, starting from the average values of parameters determined for the 9*H*-amino tautomer of adenine (Voet &

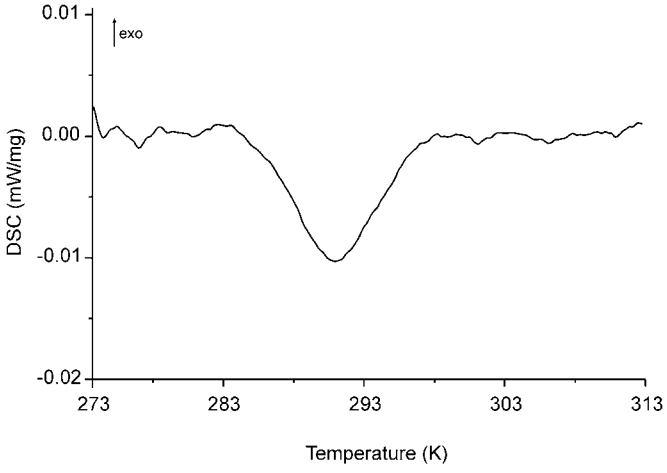

Figure 6
Kinetin dihydrogenphosphate DSC curve (fragment).

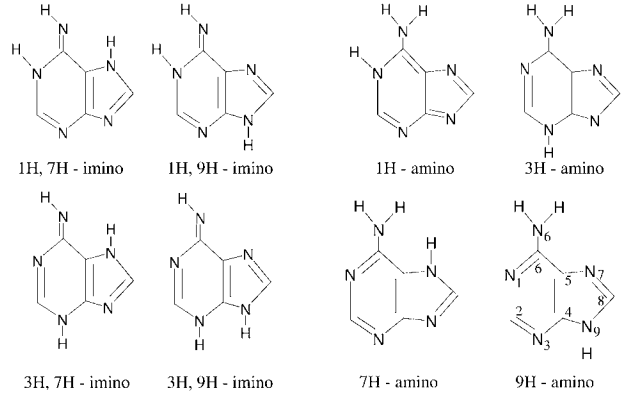

Figure 7
Tautomeric forms of the adenine molecule.

Table 4
Parameters (°) determining the conformation of the kinetin cation.

The torsion angles are defined as in Korszun *et al.* (1989).

	Kinetin *A* temperature 115 K	Kinetin *B* temperature 115 K	Kinetin temperature 293 K
Torsion angles			
C12—C11—C10—N6 (φ_1)	99.3 (2)	95.3 (2)	98.20 (15)
C6—N6—C10—C11 (φ_2)	91.5 (2)	93.5 (2)	92.95 (12)
N1—C6—N6—C10 (φ_3)	10.0 (2)	6.0 (2)	6.77 (13)
Angle between the planes of adenine and furfural residues	83.52 (7)	79.54 (7)	78.63 (5)
Angle of the bend of the adenine residue ring	0.53 (12)	1.08 (12)	0.42 (7)

Rich, 1970). Columns 7–9 present the corresponding data from our study.

Analysis of the data obtained from the measurements performed at 293 K shows that the tautomeric form of adenine is close to the 7*H*-amino isomer protonated at N3. Only the N3—C4 and N9—C4 bonds are longer than expected. They are closer to the corresponding values for the 9*H*-amino tautomer protonated at N1. Similar discrepancies appear while analysing the bond angles. The values of the C2—N3—C4 and C4—N9—C8 angles fit the geometry of the 9*H*-amino tautomer better than the geometry of any other one. Finally, a hypothesis of the dynamic equilibrium between the two isomers can be formed: the 7*H*-amino form protonated at N3, which is the dominant form, and the 9*H*-amino form. This equilibrium is strictly related to the distribution of H atoms in the hydrogen-bond network.

The conformation of the kinetin molecule is determined by the torsion angles φ_1, φ_2 and φ_3 (Table 4). The values determined for the kinetin cation in the crystal under consideration are close to those known from the other data (Korszun *et al.*, 1989). Also the dihedral angle between the plane of the adenine ring and the plane of the furfuryl ring, 78.63°, fits the range (63–108°) defined for the N^6-substituted adenine compounds (Korszun *et al.*, 1989; Stanley *et al.*, 2003).

While decreasing the crystal temperature two symmetrically inequivalent cations of kinetin appear in the new structural form. The analysis of the parameters characterizing the adenine residue of kinetin *A* (Table 3) shows that the cation has a form close to the 7*H*-amino tautomer which is protonated in the N3 position. With regard to the conformation, only the torsion angle φ_3 increases from 6.77 to 10°, which in turn causes an increase in the dihedral angle between the adenine and furfuryl rings up to 83.52° (see Table 4).

The structure of the adenine residue in kinetin *B* is much more complicated. On the basis of the data presented in Table 3, it can be concluded that it is close to the corresponding structure of the doubly protonated adenine molecule (with the protonation side at the N7 and N3 atoms). There are, however, some discrepancies concerning the N1—C2 bond length and the C2—N1—C6 angle. The values of both these parameters fit the non-protonated forms of 7*H*-amino and 9*H*-amino isomers better. The conformation of kinetin B is slightly different from that of kinetin *A* and close to that determined at 293 K.

The difference between the two inequivalent kinetin cations *A* and *B* is also manifested by a change in the planarity of the adenine ring. It is well known that the pseudoaromatic character of the purine molecule causes a small bending of the adenine ring around the C4—C5 bond, which is described by the dihedral angle between the pyrimidine and imidazole rings. In the crystal of adenine hydrochloride hemihydrate, where adenine appears as the 9*H*-amino tautomer protonated at the N1 atom, the dihedral angle is 0.79 (3)° (Cunane & Taylor, 1993). This angle increases with the further protonation of adenine at the N7 atom to 0.87°, as observed in the adenine dihydrochloride crystal (Kistenmacher & Shigematsu, 1974*b*). According to our data the adenine residue in cation *A* bends by 0.53° (Table 4). However, for cation *B* its value increases to 1.08°. At high temperatures, where the adenine residue has the form of the 7*H*-amino tautomer protonated at the N3 atom the bending is again described by the angle 0.42°.

4. Summary

Studies of the crystal structure of kinetin dihydrogenphosphate have given us an opportunity to analyse several important features of the adenine residue from the compounds of the cytokinin family. We have noticed that the substitution of the adenine molecule at the N6 atom causes a substantial change not only in biological activity, but also in its chemical and physical characteristics.

Our analysis has confirmed specific characteristics of the N1 atom in this group of compounds. In the kinetin dihydrogenphosphate crystal this is the only N atom not involved in the hydrogen-bond network. The same is observed in the crystals of kinetin hydrochloride (Stanley *et al.*, 2003) and N^6-benzyladenine hydrobromide (Langer *et al.*, 1979). At the same time this feature of the kinetin molecule strongly influences the transformation of the tautomeric forms of the adenine residue, which could be well seen in the low-temperature phase of the kinetin dihydrogenphosphate crystal. Even in the state of diprotonation, which we have assigned to the kinetin cation *B*, the protons are bound to the N3, N7 and N9 atoms.

On the basis of the analysis presented it can be concluded that the exchange of the tautomeric forms of adenine residues in the kinetin molecule in the presence of orthophosphoric acid is not unequivocal. The dominant form is the 7*H*-amino tautomer protonated at the N3 atom. The structural phase transition, which takes place at 291 K, is closely connected with the redistribution of H atoms in the hydrogen-bond network. The molecular dynamics within this network determines the dynamic equilibrium between the tautomeric states of the adenine residue.

Authors would like to thank Professor Jan Barciszewski for very helpful discussions.

References

Balasubramanian, T., Muthiah, P. T., Saravanan, A. & Mazumdar, S. K. (1996). *J. Inorg. Biochem.* **63**, 175–181.

Barciszewski, J., Rattan, S. I. S., Siboska, G. & Clark, B. F. C. (1999). *Plant Sci.* **148**, 37–45.

Barciszewski, J., Siboska, G., Rattan, S. I. S. & Clark, B. F. C. (2000). *Plant Growth Reg.* **32**, 257–265.

Cohen, B., Hare, P. M. & Kohler, B. (2003). *J. Am. Chem. Soc.* **125**, 13594–13601.

Cunane, L. M. & Taylor, M. R. (1993). *Acta Cryst.* B**49**, 524–530.

Hingerty, B. E., Einstein, J. R. & Wei, Ch. H. (1981). *Acta Cryst.* B**37**, 140–147.

Kistenmacher, T. J. & Shigematsu, T. (1974*a*). *Acta Cryst.* B**30**, 166–168.

Kistenmacher, T. J. & Shigematsu, T. (1974*b*). *Acta Cryst.* B**30**, 1528–1533.

Korszun, Z. R., Knight, C. & Chen, C.-M. (1989). *FEBS Lett.* **243**, 53–56.

Krzaczkowska, J., Gierszewski, J. & Ślósarek, G. (2004). *J. Sol. Chem.* **33**, 395–406.

Langer, V. & Huml, K. (1978*a*). *Acta Cryst.* B**34**, 1157–1163.

Langer, V. & Huml, K. (1978*b*). *Acta Cryst.* B**34**, 1881–1884.

Langer, V., Huml, K. & Lessinger, L. (1978). *Acta Cryst.* B**34**, 2229–2234.

Langer, V., Huml, K. & Zachova, J. (1979). *Acta Cryst.* B**35**, 1148–1152.

Miller, C. O., Skoog, F., van Saltza, M. H. & Strong, F. M. (1955). *J. Am. Chem. Soc.* **77**, 1392.

Miller, C. O., Skoog, F., Okumura, F. S., van Saltza, M. H. & Strong, F. M. (1956). *J. Am. Chem. Soc.* **78**, 1375–1380.

Parvez, M. & Birdsall, W. J. (1990). *Acta Cryst.* C**46**, 1775–1778.

Raghunathan, S. & Pattabhi, V. (1981). *Acta Cryst.* B**37**, 1670–1673.

Sheldrick, G. M. (1997). *SHELXL*97. University of Göttingen, Germany.

Shieh, H.-S. & Voet, D. (1975). *Acta Cryst.* B**31**, 2192–2201.

Soriano-Garcia, M. & Parthasarathy, R. (1977). *Acta Cryst.* B**33**, 2674–2677.

Stanley, N., Muthiah, P. T. & Geib, S. J. (2003). *Acta Cryst.* C**59**, o27–o29.

Taylor, R. & Kennard, O. (1982). *J. Mol. Struct.* **78**, 1–28.

Umadevi, B., Stanley, N., Muthiah, P. Th., Bocelli, G. & Cantoni, A. (2001). *Acta Cryst.* E**57**, o881–o883.

Voet, D. & Rich, A. (1970). *Prog. Nucl. Acid Res. Mol. Biol.* **10**, 183-265.